9th International Kimberlite Conference Extended Abstract No. 9IKC-A-00072, 2008

Syngenetic graphite inclusions in diamond: Experimental data.

Alexander F. Khokhryakov, Denis V. Nechaev, Alexander G. Sokol, Yuri N. Palyanov
Institute of Geology and Mineralogy SB RAS, Novosibirsk, Russian Federation

The occurrence of graphite inclusions in natural diamond crystals is commonly accounted for by later graphitization of diamond (Harris, 1972) or crystallization of thermodynamically stable graphite prior to diamond growth (Bulanova, 1995, Nasdala et al., 2005). The possibility of formation of syngenetic graphite inclusions in diamond has not been considered. Taking into account experimental proofs of joint crystallization of diamond and graphite in the diamond stability field (Sokol et al., 2001, Pal'yanov et al., 2002), we performed an experimental study of graphite inclusions formation in diamond during the growth and annealing processes. Experiments on crystallization and annealing of diamond were carried out using a "split-sphere" type multi-anvil apparatus at P=5.7–7.5 GPa, T=1400–2500°C. Details on the high-pressure sell design, calibration of pressures and temperatures were presented in our previous works (Pal'yanov et al., 1999, Pal'yanov et al., 2002). Synthetic diamond crystals were also annealed at 1500°C in vacuum (10^{-5} atm.). As a result, graphite inclusions of three genetic types (protogenetic, syngenetic and epigenetic) were experimental produced in diamond. Initial graphite, crystallized diamonds and graphite inclusions were analyzed using optical and scanning electron microscopes. Raman spectra were measured using an OMARS–89 Raman microspectrometer with excitation by the green line of an argon–ion laser (λ=514.5 nm).

Protogenetic inclusions.

Diamond crystals with protogeneric graphite inclusions were produced in the Na_2CO_3+C system at P=5.7–7.5 GPa, T=1420–1800°C, time – from 0.5 to 2 h (Pal'yanov et al., 2002) and in the NaCl+C system at P=7.5 GPa, T=1800°C, time – 20 h. In the NaCl+C system growing diamond crystals entrap isometric fragments of the initial non-reacted graphite. Diamond crystallization in the Na_2CO_3+C system proceeds through a film of the melt with thickness up to 50 μm. This carbonate melt film contains large amount of not completely dissolved graphite, which is trapped by growing diamond crystals. Diamond growth layers contain large number of small flaky graphite inclusions up to 5 μm in size (Fig. 1).

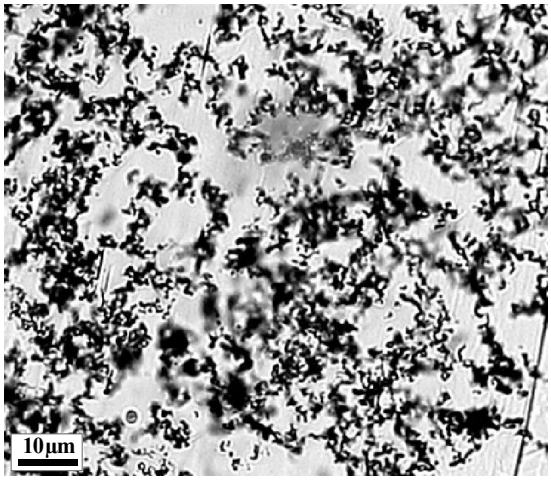

Fig. 1. Optical micrograph (transmitted light) of graphite inclusions in diamond layer grown on the {100} face of the seed crystal (Na_2CO_3+C system).

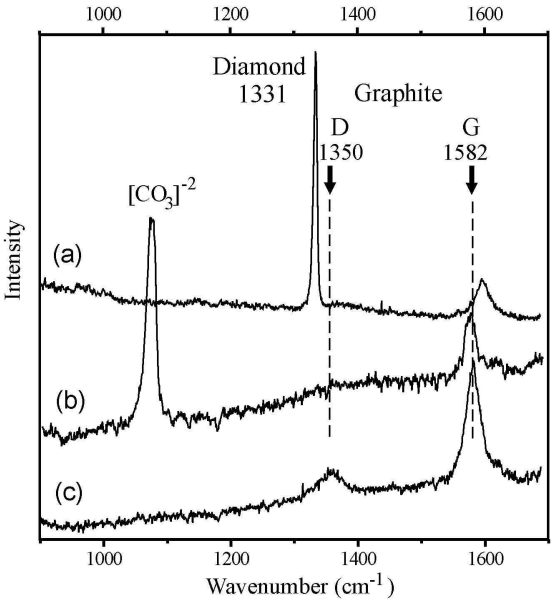

Fig. 2. Raman spectra of the black diamond crystals (a) and carbonate film between diamond and graphite (b) from run at 5.7 GPa and 1420°C in the Na_2CO_3+C system. (c) Raman spectrum of initial graphite.

From the shift of the Raman bands of graphite inclusions in diamond the residual pressure in these inclusions is estimated (Fig. 2). Depending on the P,T parameters of entrapment the residual pressure is found to be in the range from 2.6 to 3.4 GPa.

Syngenetic inclusions.

Plate-like graphite inclusions with sizes up to 30 μm and orientation along the {111} diamond faces were found in diamond crystals grown in water-containing silicate (Sokol, Pal'yanov, 2008), water-containing chloride (Palyanov et al., 2007) and carbonate-silicate systems at 7.5 GPa and 1600°C for 15–40 h (Fig. 3). Graphite inclusions of hexagonal or rounded shape were also present diamond layers grown on the seed crystals.

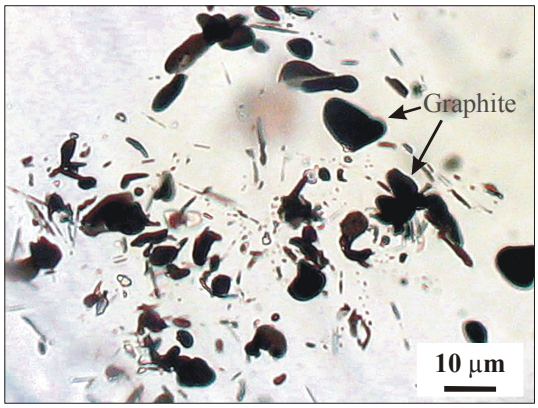

Fig. 3. Optical micrograph (transmitted light) of graphite inclusions in diamond layer grown on the {111} face of the seed crystals from the SiO_2+H_2O+C system.

No strains or cracks were revealed around the graphite inclusions. Metastable graphite, quench carbon and graphite inclusions in diamonds were studied using Raman spectroscopy (Fig. 4). It was found that metastable graphite corresponded to highly ordered graphite (HOPG). The Raman spectra exhibited only G band at 1582 cm^{-1}. For the quench carbon broad D and G bands of similar intensities were found in the Raman spectra, indicating a low-ordered structure. Graphite inclusions in diamonds corresponded to highly ordered graphite with the G band at 1591 cm^{-1}. The shift of the G band position for 11 cm^{-1} to higher frequencies can be accounted for by compressive strains in the inclusions, which is characteristic for most inclusions in diamond. Using the available data on the pressure-induced shift of the G band of graphite, residual pressure in the inclusions was calculated to be approximately 2.3 GPa.

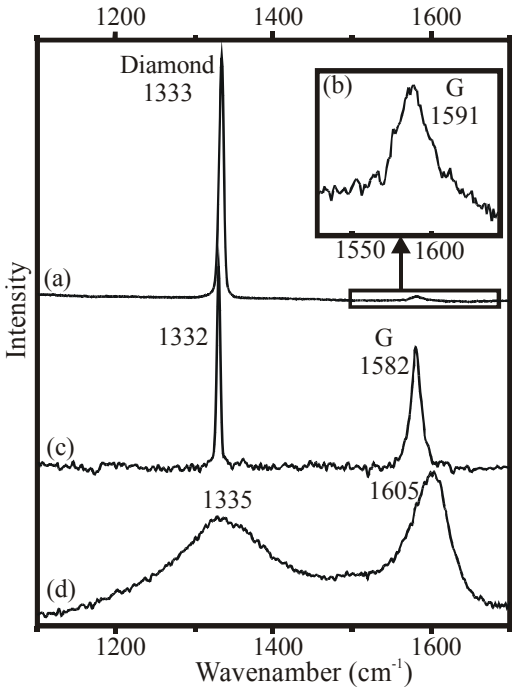

Fig. 4. Raman spectra of graphite inclusion (a,b) in diamond (Mg_2SiO_4+H_2O+C system). (c) Metastable graphite on {111} face diamond from the NaCl+H_2O+C system. (d) Quench carbon from run in the SiO_2+H_2O+C system.

Epigenetic inclusions.

Synthetic diamond crystals produced in metal-carbon systems were used for annealing. Crystals contained clusters of pin-point inclusions of less than 1 μm in size, which were located in the regions of the beginning of growth.

After annealing of diamond crystals at T=1500°C for 30 min in vacuum, black hexagonal plates were found to form around the pin-point inclusions (Fig. 5). The plates were oriented along the {111} faces and generated considerable strains in diamond. Raman spectra revealed two broad bands with maxima at 1000–1100 cm^{-1} and 1450 cm^{-1} (Fig. 6 a, b), that correspond to the initial stage of the polymorphic diamond–to–graphite transition (diamond amorphization). The first band at 1000–1100 cm^{-1} is designated T–band and represents sp^3–hybridized carbon phases of amorphous diamond. The second band at 1450 cm^{-1} is supposed for sp^2–bonds with the shortest bond length (Ferrari, Robertson, 2004).

Experiments on high–pressure annealing of diamond were carried out using multi–anvil apparatus at P=7.0–7.5 GPa and T=2300–2500°C. At high pressure and temperature in the graphite stability field, surface graphitization of diamond with formation of large plates of ordered graphite along the {111} faces was observed. Raman spectra of the samples are shown in Fig. 6 c, d.

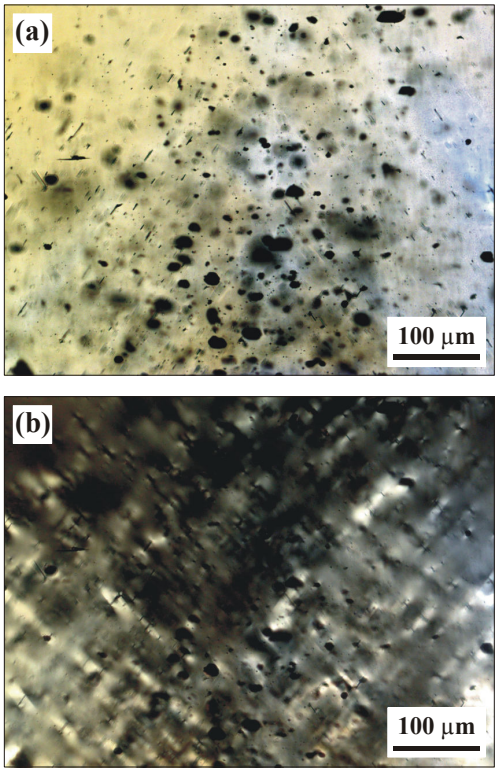

Fig. 5. Black hexagonal plates appeared around the pin–point inclusions in diamond crystal after heating in vacuum (view along [110]). (a) Non–polarized and (b) polarized light images.

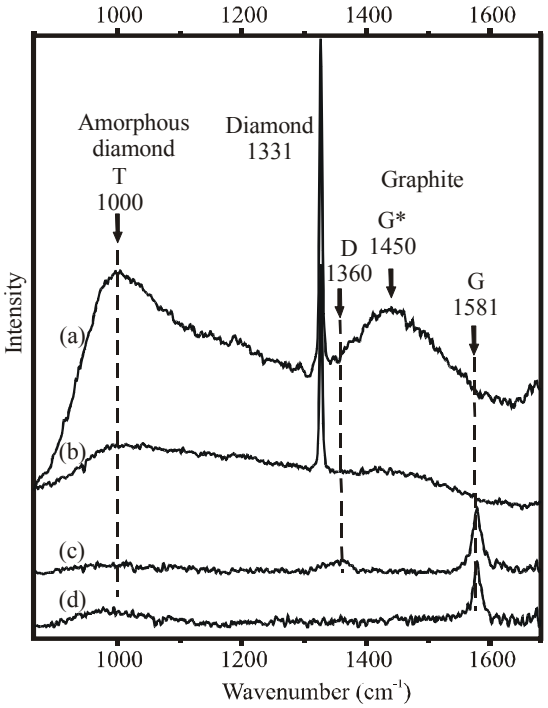

Fig. 6. Raman spectra of diamond after high-temperature treatment experiments: (a) black plates in diamond and (b) diamond around the black plates after annealing in vacuum. (c) Graphite in cracks and (d) graphite on {111} face diamond crystal after HTHP annealing.

Thus, the results obtained in this study provide an experimental proof for the possibility of formation of protogenetic, syngenetic and epigenetic graphite inclusions in diamond via three different mechanisms. Graphite inclusions in diamond can form not only in the field of thermodynamic stability of graphite prior or after diamond crystallization, but also in the field of diamond stability as a result of joint crystallization. The obtained experimental data on the formation of syngenetic graphite inclusions in diamond should be taken into consideration for interpreting genesis of graphite inclusions in natural diamond. The specific features of inclusions' morphology, Raman spectra and strain patterns around the graphite inclusions in natural diamonds can be considered as indicators of the particular formation mechanism.

This work was supported by the Russian Foundation for Basic Research (grant 06-05-64595).

References:

Bulanova, G.P., 1995. Formation of diamond. Journal of Geochemical Exploration, 53, 1-23.

Ferrari, A.C., Robertson, J., 2004. Raman spectroscopy of amorphous, nanostructured, diamond-like carbon, and nanodiamond. Phil. Trans. R. Soc. Lond. A, 362, 2477-2512.

Harris, J.W., 1972. Black material on mineral inclusions and internal fracture planes in diamond. Contr. Mineral and Petrol., 35, 22-33.

Nasdala, L., Hofmeister, W., Harris, J.W., Glinnemann, J., 2005. Growth zoning and strain patterns inside diamond crystals as revealed by Raman maps. American Mineralogist, 90, 745-748.

Pal'yanov, Yu.N., Sokol, A.G., Borzdov, Yu.M., Khokhryakov, A.F., Sobolev N.V., 1999. The diamond growth from Li_2CO_3, Na_2Co_3, K_2CO_3 and Cs_2CO_3 solvent-catalysts at P=7 GPa and T=1700-1750°C. Diamond Relat. Mater., 8, 1118-1124.

Pal'yanov, Yu.N., Sokol, A.G., Borzdov, Yu.M., Khokhryakov, A.F., 2002. Fluid-bearing alkaline carbonate melts as the medium for the formation of diamond in the Earth's mantle: an experimental study. Lithos, 60, 145-159.

Pal'yanov, Yu.N., Shatsky, V.S., Sokol, A.G., Sobolev N.V., 2007. The role of mantle ultrapotassic fluids in diamond formation. PNAS, 104, 9122-9127.

Sokol, A.G., Pal'yanov, Yu.N., Pal'yanova, G.A., Khokhryakov, A.F., Borzdov, Yu.M., 2001. Diamond and graphite crystallization from COH fluids under high pressure and high temperature conditions. Diamond Relat. Mater., 10, 2131-2136.

Sokol, A.G., Pal'yanov, Yu.N., 2008. Diamond formation in the system $MgO-SiO_2-H_2O-C$ at 7.5 GPa and 1600°C. Contrib. Mineral. Petrol., 155, 33-43.